

# Robust Design of Transmit Waveform and Receive Filter For Colocated MIMO Radar

Wei Zhu and Jun Tang

**Abstract**—We consider the problem of angle-robust joint transmit waveform and receive filter design for colocated Multiple-Input Multiple-Output (MIMO) radar, in the presence of signal-dependent interferences. The design problem is cast as a max-min optimization problem to maximize the worst-case output signal-to-interference-plus-noise-ratio (SINR) with respect to the unknown angle of the target of interest. Based on rank-one relaxation and semi-definite programming (SDP) representation of a nonnegative trigonometric polynomial, a cyclic optimization algorithm is proposed to tackle this problem. The effectiveness of the proposed method is illustrated via numerical examples.

**Index Terms**—MIMO radar, optimization, receive filter, robust design, waveform design.

## I. INTRODUCTION

Due to many advantages over conventional phased-array radar [1]–[4], multiple-input-multiple-output (MIMO) radar has been widely studied over the last decade. For both colocated [2] and distributed MIMO radar [5], one of the most crucial problems is how to design probing signals properly. Existing design approaches can mainly be classified into five categories according to the criteria adopted: 1) optimizing the radar ambiguity function [6], [7]; 2) matching a desired beam-pattern [8]–[11]; 3) optimizing the detection or estimation performance based on information theory [12]–[15]; 4) optimizing an estimation-oriented lower bound (e.g., Cramér-Rao bound [16] and Reuven-Messer bound [17]) and 5) joint transmit waveform and receive filter design to maximize the signal-to-interference-plus-noise-ratio (SINR) [18]–[21].

This letter focuses on the last design approach for colocated MIMO radar. In this design framework, joint transmit and receive beamforming is investigated in [19] for an active array in the presence of signal-dependent interference. A sequential optimization algorithm is proposed to maximize the output SINR. In [20], joint transmit waveform and receive filter design is considered under the constant modulus and similarity constraint. Both works rely on exact knowledge of target and interferences. Indeed, the angle and INR of interferences can be obtained from knowledge-aided methods or estimated through previous scans of the space in high INR cases [22], [23]. The known target angle assumption can be applied to the confirmation of an initial detection at some angle bin [24]. However, there are other situations where the target angle is unknown (e.g., weak target embedded in strong interferences), and the SINR should be averagely optimized over the uncertain area to avoid beampattern loss [4]. Hence, angular-robust

design must be considered and the robust design can also be used as an initial step for cognitive detection. In previous works [24], [25], robust waveform design has been studied for interpulse (or intrapulse) coding in radar by considering the unknown Doppler shift of target. Motivated by these works, we consider the problem of angular-robust design for colocated MIMO radar in the presence of signal-dependent interferences, which are induced by the interaction of transmit waveform with unwanted scatters. Based on the SINR criterion, transmit waveform and receive filter are jointly optimized to maximize the worst-case output SINR. Since the resulting problem is non-convex, cyclic optimization [26] and semi-definite relaxation (SDR) [27] are used to solve it. Although the cyclic optimization converges to a locally optimal solution, it still can yield a good enough solution with higher worst-case SINR than the non-robust design, as illustrated in section IV. This is fundamentally different from the optimization problem in parameter estimation, in which the local convergence may significantly deteriorate the accuracy of estimation. SDR is a powerful approximation technique to solve a host of difficult non-convex problems with rank constraints. It is commonly used in radar signal processing problems, e.g., [22]–[25].

**Notations:** Matrices are denoted by bold capital letters, and vectors by bold lowercase letters.  $(\cdot)^T$ ,  $(\cdot)^c$  and  $(\cdot)^H$  denote the transpose, conjugate and conjugate transpose, respectively.  $\|\cdot\|$  denotes Euclidean norm.  $\otimes$  denotes Kronecker product.  $I_L$  means  $L \times L$  identity matrix.  $\mathbb{R}$  and  $\mathbb{C}$  denotes the sets of all real numbers and complex numbers, respectively.  $\delta(\cdot)$  represents Kronecker delta function.  $\text{vec}(\cdot)$  denotes vectorization operator.  $\text{Re}\{\cdot\}$  denotes the real part of the argument.

## II. PROBLEM FORMULATION

Consider a colocated MIMO radar system equipped with  $N_T$  transmitters and  $N_R$  receivers. Both the transmit and receive arrays are assumed to be uniform linear arrays with half-wavelength element-separation. Let  $\mathbf{S} \in \mathbb{C}^{N_T \times N}$  denote the transmitted waveform matrix, where  $N$  is the number of samples in the duration of the transmitted waveform. For a particular range cell of interest, the received waveform matrix  $\mathbf{Y} \in \mathbb{C}^{N_R \times N}$  from  $N_R$  receivers is corrupted by  $K$  signal-dependent interferences (e.g., other targets in a multi-target scenario [23]) from adjacent range cells with the additional noise, and is modeled as

$$\mathbf{Y} = \alpha_0 \mathbf{a}_r(\theta_0) \mathbf{a}_t(\theta_0)^T \mathbf{S} + \sum_{k=1}^K \alpha_k \mathbf{a}_r(\theta_k) \mathbf{a}_t(\theta_k)^T \mathbf{S} \mathbf{J}_{r_k} + \mathbf{N}$$

where

The authors are with the Department of Electronic Engineering, Tsinghua University, Beijing, 100084, China (email: zhuwei11@mails.tsinghua.edu.cn, tangj\_ce@mail.tsinghua.edu.cn).

- $\alpha_0$  and  $\alpha_k$  are the complex amplitudes of the target and the  $k$ -th interference source, respectively.
- $\theta_0$  and  $\theta_k$  are the direction of arrivals (DOA) of the target and the  $k$ -th interference source, respectively.
- $\mathbf{a}_r(\theta) \in \mathbb{C}^{N_R \times 1}$  is the receive steering vector defined by  $\mathbf{a}_r(\theta) \triangleq [1, e^{j\pi \sin(\theta)}, \dots, e^{j\pi(N_R-1)\sin(\theta)}]^T$ .
- $\mathbf{a}_t(\theta) \in \mathbb{C}^{N_T \times 1}$  is the transmit steering vector defined by  $\mathbf{a}_t(\theta) \triangleq [1, e^{j\pi \sin(\theta)}, \dots, e^{j\pi(N_T-1)\sin(\theta)}]^T$ .
- $\mathbf{J}_{r_k}, r_k \in \{-N+1, \dots, -1, 0, 1, \dots, N-1\}$  is an  $N$ -by- $N$  shift matrix with  $(l_1, l_2)$ -th element  $\mathbf{J}_{r_k}(l_1, l_2) \triangleq \delta(l_1 - l_2 - r_k)$ .  $r_k$  is the range cell index of the  $k$ -th interference source relative to the range cell of interest.
- $\mathbf{N}$  is spatially and temporally white circularly symmetric complex Gaussian noise with mean zero and variance  $\sigma^2$ .

Let  $\mathbf{y} = \text{vec}(\mathbf{Y})$ ,  $\mathbf{s} = \text{vec}(\mathbf{S})$  and  $\mathbf{n} = \text{vec}(\mathbf{N})$ . The vectorization form of the measurement model is given by

$$\mathbf{y} = \alpha_0 \mathbf{A}(\theta_0) \mathbf{s} + \sum_{k=1}^K \alpha_k \mathbf{B}(\theta_k) \mathbf{s} + \mathbf{n} \quad (1)$$

where  $\mathbf{A}(\theta_0) = \mathbf{I}_N \otimes [\mathbf{a}_r(\theta_0) \mathbf{a}_t(\theta_0)^T]$  and  $\mathbf{B}(\theta_k) = \mathbf{J}_{r_k}^T \otimes [\mathbf{a}_r(\theta_k) \mathbf{a}_t(\theta_k)^T]$ . The SINR at the output of the receive filter  $\mathbf{w} \in \mathbb{C}^{N_R N \times 1}$  is given by

$$\mathcal{X}(\mathbf{s}, \mathbf{w}, \theta_0) = \frac{\text{SNR} |\mathbf{w}^H \mathbf{A}(\theta_0) \mathbf{s}|^2}{\mathbf{w}^H \Sigma_I(\mathbf{s}) \mathbf{w} + \mathbf{w}^H \mathbf{w}} \quad (2)$$

where  $\Sigma_I(\mathbf{s}) = \sum_{k=1}^K \text{INR}_k \mathbf{B}(\theta_k) \mathbf{s} \mathbf{s}^H \mathbf{B}(\theta_k)^H$  with the signal-to-noise-ratio (SNR) of target and the interference-to-noise-ratio (INR) of  $k$ -th interference defined as  $\text{SNR} \triangleq \mathbb{E}\{|\alpha_0|^2\} / \sigma^2$  and  $\text{INR}_k \triangleq \mathbb{E}\{|\alpha_k|^2\} / \sigma^2$ , respectively.

We assume that the angle and the INR of the interferences are all known or previously estimated, as with prior works [19], [20], [23]. We assume that the angle of target under test is known to lie in an angular sector  $\Omega = [\theta_C - \Delta\theta, \theta_C + \Delta\theta]$  centred around  $\theta_C$ , where  $\Delta\theta$  indicates the level of angular uncertainty. The goal is to maximize the worst-case SINR to improve the worst-case detection performance, under the waveform energy constraint  $\|\mathbf{s}\|^2 = E$ . Therefore, the robust design of transmit waveform and receive filter can be formulated as the following max-min problem:

$$\max_{\mathbf{s}, \mathbf{w}} \min_{\theta_0 \in \Omega} \mathcal{X}(\mathbf{s}, \mathbf{w}, \theta_0) \quad \text{subject to} \quad \|\mathbf{s}\|^2 = E \quad (3)$$

Note that for the case of known target angle, (3) reduces to the optimization problem in [19].

### III. MAX-MIN ROBUST DESIGN ALGORITHM

In this section, we shall present our algorithm to solve the problem (3). To begin with, we make some mathematical transformations to the objective function of the optimization problem. Define  $\mathbf{W} \in \mathbb{C}^{N_R \times N}$  such that  $\mathbf{w} = \text{vec}(\mathbf{W})$ . Let  $\mathbf{p}(\nu) = [1, e^{j\nu}, \dots, e^{j\nu(L-1)}]^T$  with  $L = N_R + N_T - 1$  and  $\nu = \pi \sin(\theta_0)$ . Let  $\mathbf{H} = [\tilde{\mathbf{H}}_1^T, \tilde{\mathbf{H}}_2^T, \dots, \tilde{\mathbf{H}}_{N_R}^T]^T$  where  $\mathbf{H} \in \mathbb{R}^{N_R N_T \times L}$ ,  $\tilde{\mathbf{H}}_k \in \mathbb{R}^{N_T \times L}$ ,  $k = 1, \dots, N_R$ , and the  $(m, n)$ -th element of  $\tilde{\mathbf{H}}_k$  is defined by  $\tilde{\mathbf{H}}_k(m, n) \triangleq \delta(n - m - k + 1)$ . Then, one can easily show that  $\mathbf{a}_r(\theta_0) \otimes \mathbf{a}_t(\theta_0) =$

$\mathbf{H} \mathbf{p}(\nu)$ . According to the property of Kronecker products that  $\text{vec}(\mathbf{C} \mathbf{X} \mathbf{D}) = (\mathbf{D}^T \otimes \mathbf{C}) \text{vec}(\mathbf{X})$ , we can show that

$$\mathbf{w}^H \mathbf{A}(\theta_0) \mathbf{s} = (\mathbf{A}(\theta_0)^T \text{vec}(\mathbf{W}^*))^T \mathbf{s} \quad (4)$$

$$= \text{vec}(\mathbf{a}_t(\theta_0) \mathbf{a}_r(\theta_0)^T \mathbf{W}^*)^T \mathbf{s} \quad (5)$$

$$= ((\mathbf{W}^H \otimes \mathbf{I}_{N_T}) \text{vec}(\mathbf{a}_t(\theta_0) \mathbf{a}_r(\theta_0)^T))^T \mathbf{s} \quad (6)$$

$$= \mathbf{s}^T (\mathbf{W}^H \otimes \mathbf{I}_{N_T}) (\mathbf{a}_r(\theta_0) \otimes \mathbf{a}_t(\theta_0)) \quad (7)$$

$$= \text{vec}(\mathbf{S} \mathbf{W}^H)^T \mathbf{H} \mathbf{p}(\nu) \quad (8)$$

Then, it follows that  $|\mathbf{w}^H \mathbf{A}(\theta_0) \mathbf{s}|^2 = \mathbf{p}(\nu)^H \mathbf{G} \mathbf{p}(\nu)$  where

$$\mathbf{G} \triangleq \mathbf{H}^H \text{vec}(\mathbf{S} \mathbf{W}^H)^* \text{vec}(\mathbf{S} \mathbf{W}^H)^T \mathbf{H} \quad (9)$$

Let  $\mathbf{S} = [\mathbf{s}_1, \mathbf{s}_2, \dots, \mathbf{s}_N]$  and  $\mathbf{W} = [\mathbf{w}_1, \mathbf{w}_2, \dots, \mathbf{w}_N]$ . Using  $\mathbf{S} \mathbf{W}^H = \sum_{n=1}^N \mathbf{s}_n \mathbf{w}_n^H$ , we can write

$$\text{vec}(\mathbf{S} \mathbf{W}^H) = \sum_{n=1}^N \text{vec}(\mathbf{s}_n \mathbf{w}_n^H) = \sum_{n=1}^N \mathbf{w}_n^* \otimes \mathbf{s}_n \quad (10)$$

Define  $\mathbf{X} = \mathbf{s} \mathbf{s}^H$  and  $\mathbf{V} = \mathbf{w} \mathbf{w}^H$  with  $\mathbf{X} \in \mathbb{C}^{N_T N \times N_T N}$  and  $\mathbf{V} \in \mathbb{C}^{N_R N \times N_R N}$ . Partition  $\mathbf{X}$  and  $\mathbf{V}$  into a  $N$ -by- $N$  block matrix with  $(n_1, n_2)$ -th block denoted by  $\mathbf{X}_{[n_1, n_2]} \in \mathbb{C}^{N_T \times N_T}$  and  $\mathbf{V}_{[n_1, n_2]} \in \mathbb{C}^{N_R \times N_R}$ , then it follows that

$$\mathbf{G}(\mathbf{X}, \mathbf{V}) = \mathbf{H}^H \left( \sum_{1 \leq n_1, n_2 \leq N} \mathbf{V}_{[n_1, n_2]} \otimes \mathbf{X}_{[n_1, n_2]}^* \right) \mathbf{H} \quad (11)$$

where we use the notation  $\mathbf{G}(\mathbf{X}, \mathbf{V})$  to emphasize  $\mathbf{G}$  as a function of  $\mathbf{X}$  and  $\mathbf{V}$ . Moreover, using  $\mathbf{w}^H \mathbf{w} = \text{tr}(\mathbf{V}) \text{tr}(\mathbf{X}) / E$  and  $\mathbf{w}^H \Sigma_I(\mathbf{s}) \mathbf{w} = \text{tr}(\Sigma_I(\mathbf{V}) \mathbf{X})$  with  $\Sigma_I(\mathbf{V}) = \sum_{k=1}^K \text{INR}_k \mathbf{B}(\theta_k)^H \mathbf{V} \mathbf{B}(\theta_k)$ , it is easy to find that the denominator of (2) can be re-written as  $\text{tr}((\Sigma_I(\mathbf{V}) + \frac{\text{tr}(\mathbf{V})}{E} \mathbf{I}_{N_T N}) \mathbf{X})$ . Consequently, problem (3) can be recast as

$$\begin{cases} \max_{\mathbf{X}, \mathbf{V}} \min_{\nu \in \mathcal{I}} & \frac{\mathbf{p}(\nu)^H \mathbf{G}(\mathbf{X}, \mathbf{V}) \mathbf{p}(\nu)}{\text{tr} \left( \left( \Sigma_I(\mathbf{V}) + \frac{\text{tr}(\mathbf{V})}{E} \mathbf{I}_{N_T N} \right) \mathbf{X} \right)} \\ \text{subject to} & \text{tr}(\mathbf{X}) = E, \mathbf{X} \succeq \mathbf{0}, \mathbf{V} \succeq \mathbf{0} \\ & \text{rank}(\mathbf{X}) = 1, \text{rank}(\mathbf{V}) = 1 \end{cases} \quad (12)$$

where  $\mathcal{I} = [\nu_C - \Delta\nu, \nu_C + \Delta\nu]$  is the corresponding uncertain range of  $\nu$  after parameter transformation.

#### A. Optimization with respect to $\mathbf{X}$ and $\mathbf{V}$

Since the rank constraint in (12) is non-convex, we adopt the commonly-used SDR technique [27] to obtain a relaxed problem by dropping the rank-one constraint in (12):

$$\begin{cases} \max_{\mathbf{X}, \mathbf{V}} \min_{\nu \in \mathcal{I}} & \frac{\mathbf{p}(\nu)^H \mathbf{G}(\mathbf{X}, \mathbf{V}) \mathbf{p}(\nu)}{\text{tr} \left( \left( \Sigma_I(\mathbf{V}) + \frac{\text{tr}(\mathbf{V})}{E} \mathbf{I}_{N_T N} \right) \mathbf{X} \right)} \\ \text{subject to} & \text{tr}(\mathbf{X}) = E, \mathbf{X} \succeq \mathbf{0}, \mathbf{V} \succeq \mathbf{0} \end{cases} \quad (13)$$

or equivalently,

$$\begin{cases} \max_{\mathbf{U}, \mathbf{V}, t, \gamma} & t \\ \text{subject to} & \mathbf{p}(\nu)^H \mathbf{G}(\mathbf{U}, \mathbf{V}) \mathbf{p}(\nu) \geq t, \text{ for } \forall \nu \in \mathcal{I} \\ & \text{tr} \left( \left( \Sigma_I(\mathbf{V}) + \frac{\text{tr}(\mathbf{V})}{E} \mathbf{I}_{N_T N} \right) \mathbf{U} \right) = 1 \\ & \text{tr}(\mathbf{U}) = E\gamma, \gamma \geq 0 \\ & \mathbf{U} \succeq \mathbf{0}, \mathbf{V} \succeq \mathbf{0} \end{cases} \quad (14)$$



We also note that the randomized method [27] can also be used to obtain an approximate  $\mathbf{s}^*$  and  $\mathbf{w}^*$  in the non-rank-one case. Similar applications can be found in [20], [31], [32]. The synthesis algorithm based on the randomized method for our problem is shown in Algorithm 1.

---

**Algorithm 1** Synthesis algorithm based on randomized method

---

**Input:**  $\mathbf{X}^*$  and  $\mathbf{V}^*$

**Output:** A randomized approximate solution  $\mathbf{s}^*$  and  $\mathbf{w}^*$

- 1: **if**  $\text{rank}(\mathbf{V}^*) = 1$  **then**
- 2:   find  $\mathbf{w}^*$  via eigen-decomposition  $\mathbf{V}^* = \mathbf{w}^*(\mathbf{w}^*)^H$
- 3: **else**
- 4:   draw  $R$  random vectors  $\mathbf{w}_j$  from the complex Gaussian distribution  $\mathcal{CN}(\mathbf{0}, \mathbf{V}^*)$ ,  $j = 1, 2, \dots, R$
- 5:   calculate

$$\xi_j = \min_{\theta_0 \in \Omega} \frac{\mathbf{w}_j^H \mathbf{A}(\theta_0) \mathbf{X}^* \mathbf{A}(\theta_0)^H \mathbf{w}_j}{\mathbf{w}_j^H \Sigma_I(\mathbf{X}^*) \mathbf{w}_j + \mathbf{w}_j^H \mathbf{w}_j}, \quad j = 1, \dots, R$$

where  $\Sigma_I(\mathbf{X}^*) = \sum_{k=1}^K \text{INR}_k \mathbf{B}(\theta_k) \mathbf{X}^* \mathbf{B}(\theta_k)^H$ .

- 6:   let  $\mathbf{w}^* = \mathbf{w}_{j_{\max}}$  where

$$j_{\max} = \arg \max_{1 \leq j \leq R} \xi_j.$$

- 7: **end if**
- 8: **if**  $\text{rank}(\mathbf{X}^*) = 1$  **then**
- 9:   find  $\mathbf{s}^*$  via eigen-decomposition  $\mathbf{X}^* = \mathbf{s}^*(\mathbf{s}^*)^H$

10: **else**

- 11:   draw  $R$  random vectors  $\mathbf{s}_i$  from the complex Gaussian distribution  $\mathcal{CN}(\mathbf{0}, \mathbf{X}^*)$ ,  $i = 1, 2, \dots, R$

- 12:   calculate  $\bar{\mathbf{s}}_i = \frac{\sqrt{E} \mathbf{s}_i}{\|\mathbf{s}_i\|}$  and

$$\zeta_i = \min_{\theta_0 \in \Omega} \frac{|(\mathbf{w}^*)^H \mathbf{A}(\theta_0) \bar{\mathbf{s}}_i|^2}{(\mathbf{w}^*)^H \Sigma_I(\bar{\mathbf{s}}_i) \mathbf{w}^* + (\mathbf{w}^*)^H \mathbf{w}^*}, \quad i = 1, \dots, R$$

where  $\Sigma_I(\bar{\mathbf{s}}_i) = \sum_{k=1}^K \text{INR}_k \mathbf{B}(\theta_k) \bar{\mathbf{s}}_i \bar{\mathbf{s}}_i^H \mathbf{B}(\theta_k)^H$ .

- 13:   let  $\mathbf{s}^* = \bar{\mathbf{s}}_{i_{\max}}$  where

$$i_{\max} = \arg \max_{1 \leq i \leq R} \zeta_i.$$

14: **end if**

---

Prior results on the tightness of SDR [27], [33] show that for a separable SDP [27, eq. (28)] with  $P$  semi-definite variables and  $J$  constraints, there exists a rank-one optimal solution if  $J \leq P + 2$ . But this can not guarantee the existence of rank-one solution for our problem, since  $P = 3$  and  $J = 2L - 1$  for problem (17) and (18) in the form of [27, eq. (28)]. Nevertheless, we emphasize that as with in [25], one can empirically observe that both  $\mathbf{X}^*$  and  $\mathbf{V}^*$  are rank-one for most of the random initializations as along as  $\Omega \cap \Omega_c = \emptyset$ , where  $\Omega_c$  denotes the set of all interferences angles.

#### IV. NUMERICAL EXAMPLES

In this section, numerical examples are conducted to examine the performance of the proposed method. In all examples, we assume that 30 interferences are present with the range and angle pair  $(r_k, \theta_k)$  generated from all possible combinations

of  $\{-2, -1, 0, 1, 2\} \times \{-60^\circ, -50^\circ, -40^\circ, 40^\circ, 60^\circ, 70^\circ\}$ . The INR of all interferences is 30 dB.

In Fig. 1, the output SINR as a function of  $\theta_0$  for the non-robust design and the proposed robust design are compared under four different parameters. For the non-robust design, the assumed a-prior target angle is set to be  $\theta_C$  and the optimization algorithm is based on the method presented in [19]. It is shown that the robust design improves the worst-case SINR performance significantly at the cost of peak-SINR degradation. For fixed  $\Delta\theta$  and  $N$ , the superiority of robust design increases with the number of transmitters or receivers. In Fig. 2, we depict the beampattern  $P(\theta) = \frac{\|\mathbf{w}^H \mathbf{A}(\theta) \mathbf{s}\|^2}{N_R N_T \|\mathbf{w}\|^2 \|\mathbf{s}\|^2}$  for parameter settings in Fig. 1(c) and Fig. 1(d) as an example. One can observe that both robust and non-robust design can produce nulls near the DOAs of interferences. From Fig. 1 and Fig. 2, we see that when  $\Delta\theta$  is large enough relative to the beamwidth, the robust design can form a wide and flat beam over the uncertain space area to bring robustness. Both  $\mathbf{X}^*$  and  $\mathbf{V}^*$  are rank-one in this example.

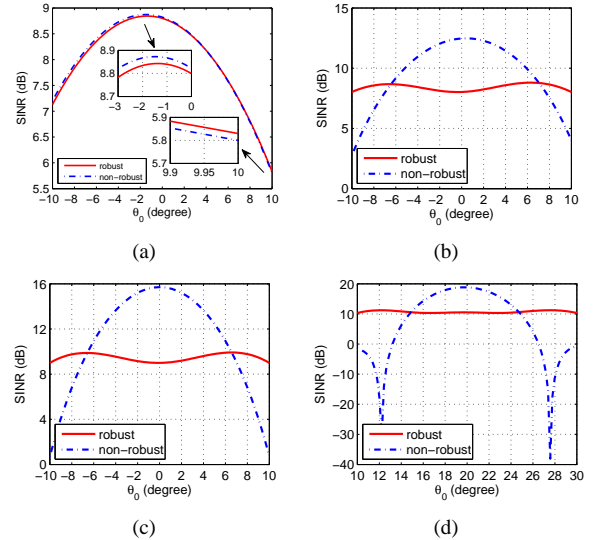


Fig. 1. Comparisons of the output SINR.  $\Delta\theta = 10^\circ$ .  $E = N = 20$ . SNR = -15dB. (a)  $N_R = N_T = 4$ ,  $\theta_C = 0^\circ$ ; (b)  $N_R = 4$ ,  $N_T = 8$ ,  $\theta_C = 0^\circ$ ; (c)  $N_R = N_T = 8$ ,  $\theta_C = 0^\circ$ ; (d)  $N_R = 8$ ,  $N_T = 16$ ,  $\theta_C = 20^\circ$ .

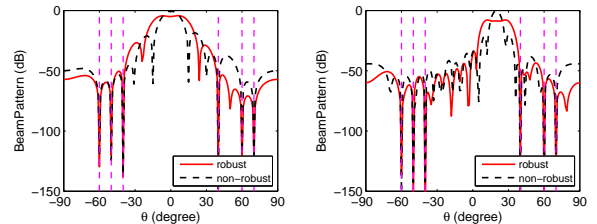


Fig. 2. Comparisons of the beampattern  $P(\theta)$ . (left)  $N_R = N_T = 8$ ,  $\theta_C = 0^\circ$ ; (right)  $N_R = 8$ ,  $N_T = 16$ ,  $\theta_C = 20^\circ$ .

In Fig. 3, we plot the worst-case SINR versus the target angle uncertainty  $\Delta\theta$ . As expected, a wider range of target angle uncertainty leads to a worse SINR. The impact of  $\Delta\theta$  on the worst-case SINR performance of non-robust design is more prominent, which suffers a sharp decline as  $\Delta\theta$  increases. This

is due to the effect of the first null near the main lobe. In this example, both  $\mathbf{X}^*$  and  $\mathbf{V}^*$  are rank-one.

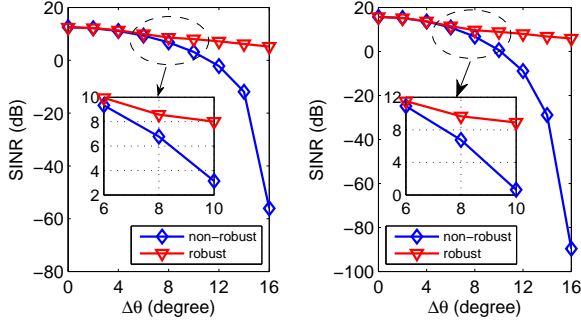


Fig. 3. The worst-case output SINR versus the angle uncertainty.  $\theta_C = 0^\circ$ .  $E = N = 20$ . SNR = -15dB. (left)  $N_R = 4$ ,  $N_T = 8$ ; (right)  $N_R = N_T = 8$ .

In Fig. 4, we investigate the effect of initial values on the cyclic optimization of  $\mathbf{X}$  and  $\mathbf{V}$ . We plot the worst-case SINR for the relaxed problem (14) under  $\Gamma = 50$  different random initializations. Four different parameter settings are considered. The cyclic optimization is stopped if either the increment of the worst-case SINR between two iterations is less than  $5 \times 10^{-3}$  or the maximum number of iterations reaches. The maximum number of iterations of the cyclic optimization is set to 150. We can see that the worst-case SINRs under different initializations are very close. Let  $\mathcal{T} = \{t^{(1)}, t^{(2)}, \dots, t^{(\Gamma)}\}$  denote the worst-case SINRs from  $\Gamma$  random initializations. We define the following metric

$$\mathcal{L} \triangleq \frac{\max(\mathcal{T}) - \min(\mathcal{T})}{\text{mean}(\mathcal{T})} \quad (22)$$

to evaluate the variation of  $\mathcal{T}$ , where  $\max(\mathcal{T})$ ,  $\min(\mathcal{T})$  and  $\text{mean}(\mathcal{T})$  denote the maximum, minimum and mean value of  $\mathcal{T}$ , respectively. The values of  $\mathcal{L}$  for the four cases are equal to 0.016, 0.0177, 0.0263 and 0.016, respectively. One can see that in our problem, the cyclic optimization is quite insensitive to the initialization.

In Fig. 5, we illustrate the performance of the synthesis algorithm in the non-rank-one case, which seldom happens in our experiments. In this example, the parameter settings are the same as in Fig. 4(c). Under a certain random initialization, the cyclic optimization provides a solution with  $\text{rank}(\mathbf{X}^*) = 2$  and  $\text{rank}(\mathbf{V}^*) = 1$ . The receive filter  $\mathbf{w}^*$  is obtained based on eigen-decomposition, and the transmit waveform  $\mathbf{s}^*$  is obtained via the synthesis algorithm. The performance of synthesis algorithm based on solving problem (20) (denoted Method 1) and the algorithm based on randomized method (denoted Method 2) are compared. We plot their corresponding SINRs as a function of  $\theta_0$  according to (2). For the Method 1, the number of DOA samples  $M$  is set to 41 and the number of iterations to solve (20) is 50. For the Method 2, the number of random samples is set to be 1000. We also plot the  $\text{SINR}_{\text{relax}}(\theta_0) \triangleq \frac{\text{SNR} \text{tr}(\mathbf{X}^* \mathbf{A}(\theta_0)^H \mathbf{V}^* \mathbf{A}(\theta_0))}{\text{tr}((\sum_I(\mathbf{X}^*) + \mathbf{I}_{N_R N}) \mathbf{V}^*)}$  as a benchmark for comparison. We can observe that their SINR performance are very close, and both synthesis algorithms yield a good solution in the non-rank-one case. We can also see that the

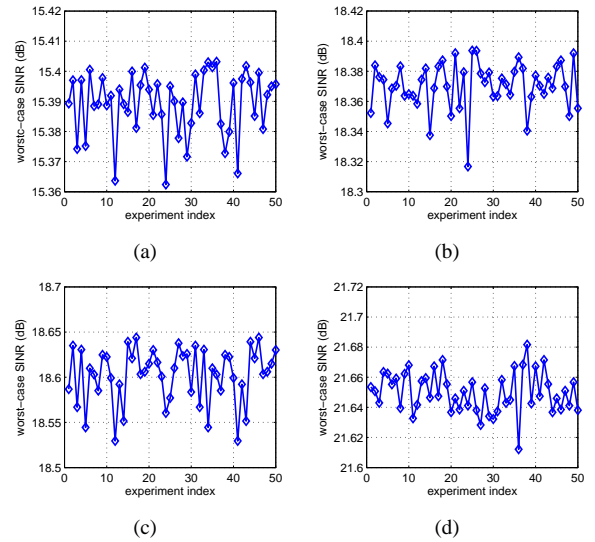


Fig. 4. The effect of initial values on cyclic optimization.  $E = N_T N$ , SNR =  $1/L$ ,  $\theta_C = 0^\circ$  and  $\Delta\theta = 10^\circ$ . (a)  $N_R = N_T = 4$ ,  $N = 10$ ; (b)  $N_R = N_T = 4$ ,  $N = 20$ ; (c)  $N_R = 4$ ,  $N_T = 8$ ,  $N = 10$ . (d)  $N_R = 4$ ,  $N_T = 8$ ,  $N = 20$ .

SINR curve of Method 1 matches well with  $\text{SINR}_{\text{relax}}(\theta_0)$ . The worst-case SINRs for Method 1, Method 2 and  $\text{SINR}_{\text{relax}}(\theta_0)$  are 18.478 dB, 18.394 dB 18.526 dB, respectively.

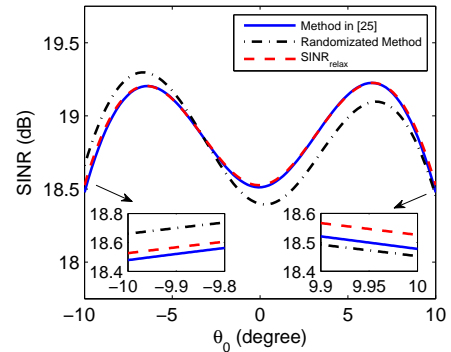


Fig. 5. The SINR performance of the synthesis algorithm.

## V. CONCLUSIONS

A method for angular-robust joint design of transmit waveform and receive filter is proposed to maximize the worst-case SINR performance. The proposed method exhibits a considerable performance increment over the non-robust design via numerical examples. Future work will concentrate on the robust design with respect to the interferences uncertainty.

## REFERENCES

- [1] J. Li and P. Stoica, *MIMO Radar Signal Processing*. A John Wiley Sons, INC, 2008.
- [2] —, “MIMO radar with colocated antennas,” *IEEE Signal Process. Mag.*, vol. 24, no. 5, pp. 106–114, Sept 2007.
- [3] E. Fishler, A. Haimovich, R. Blum, L. Cimini, D. Chizhik, and R. Valenzuela, “Spatial diversity in radars-models and detection performance,” *IEEE Trans. Signal Process.*, vol. 54, no. 3, pp. 823–838, March 2006.
- [4] I. Bekkerman and J. Tabrikian, “Target detection and localization using MIMO radars and sonars,” *IEEE Trans. Signal Process.*, vol. 54, no. 10, pp. 3873–3883, Oct 2006.

- [5] A. Haimovich, R. Blum, and L. Cimini, "MIMO radar with widely separated antennas," *IEEE Signal Process. Mag.*, vol. 25, no. 1, pp. 116–129, 2008.
- [6] G. San Antonio, D. Fuhrmann, and F. Robey, "MIMO radar ambiguity functions," *IEEE J. Sel. Topics Signal Process.*, vol. 1, no. 1, pp. 167–177, June 2007.
- [7] C.-Y. Chen and P. Vaidyanathan, "MIMO radar ambiguity properties and optimization using frequency-hopping waveforms," *IEEE Trans. Signal Process.*, vol. 56, no. 12, pp. 5926–5936, Dec 2008.
- [8] P. Stoica, J. Li, and Y. Xie, "On probing signal design for MIMO radar," *IEEE Trans. Signal Process.*, vol. 55, no. 8, pp. 4151–4161, Aug 2007.
- [9] D. Fuhrmann and G. San Antonio, "Transmit beamforming for MIMO radar systems using signal cross-correlation," *IEEE Trans. Aerosp. Electron. Syst.*, vol. 44, no. 1, pp. 171–186, January 2008.
- [10] M. Soltanalian, H. Hu, and P. Stoica, "Single-stage transmit beamforming design for MIMO radar," *Signal Processing*, vol. 102, pp. 132–138, 2014.
- [11] A. Khabbazi-basmenj, A. Hassanien, S. A. Vorobyov, and M. W. Morency, "Efficient transmit beamspace design for search-free based doa estimation in MIMO radar," *IEEE Trans. Signal Process.*, vol. 62, no. 6, pp. 1490–1500, 2014.
- [12] Y. Yang and R. Blum, "MIMO radar waveform design based on mutual information and minimum mean-square error estimation," *IEEE Trans. Aerosp. Electron. Syst.*, vol. 43, no. 1, pp. 330–343, January 2007.
- [13] A. Leshem, O. Naparstek, and A. Nehorai, "Information theoretic adaptive radar waveform design for multiple extended targets," *IEEE J. Sel. Topics Signal Process.*, vol. 1, no. 1, pp. 42–55, June 2007.
- [14] B. Tang, J. Tang, and Y. Peng, "MIMO radar waveform design in colored noise based on information theory," *IEEE Trans. Signal Process.*, vol. 58, no. 9, pp. 4684–4697, 2010.
- [15] M. Akcakaya and A. Nehorai, "MIMO radar detection and adaptive design under a phase synchronization mismatch," *IEEE Trans. Signal Process.*, vol. 58, no. 10, pp. 4994–5005, 2010.
- [16] J. Li, L. Xu, P. Stoica, K. Forsythe, and D. Bliss, "Range compression and waveform optimization for MIMO radar: A cramer-rao bound based study," *IEEE Trans. Signal Process.*, vol. 56, no. 1, pp. 218–232, Jan 2008.
- [17] W. Huleihel, J. Tabrikian, and R. Shavit, "Optimal adaptive waveform design for cognitive MIMO radar," *IEEE Trans. Signal Process.*, vol. 61, no. 20, pp. 5075–5089, Oct 2013.
- [18] C.-Y. Chen and P. Vaidyanathan, "MIMO radar waveform optimization with prior information of the extended target and clutter," *IEEE Trans. Signal Process.*, vol. 57, no. 9, pp. 3533–3544, 2009.
- [19] J. Liu, H. Li, and B. Himed, "Joint optimization of transmit and receive beamforming in active arrays," *IEEE Signal Process. Lett.*, vol. 21, no. 1, pp. 39–42, Jan 2014.
- [20] G. Cui, H. Li, and M. Rangaswamy, "MIMO radar waveform design with constant modulus and similarity constraints," *IEEE Trans. Signal Process.*, vol. 62, no. 2, pp. 343–353, Jan 2014.
- [21] S. Imani and S. Ghorashi, "Transmit signal and receive filter design in co-located MIMO radar using a transmit weighting matrix," *IEEE Signal Process. Lett.*, vol. 22, no. 10, pp. 1521–1524, Oct 2015.
- [22] A. Aubry, A. DeMaio, A. Farina, and M. Wicks, "Knowledge-aided (potentially cognitive) transmit signal and receive filter design in signal-dependent clutter," *IEEE Trans. Aerosp. Electron. Syst.*, vol. 49, no. 1, pp. 93–117, Jan 2013.
- [23] A. Duly, D. Love, and J. Krogmeier, "Time-division beamforming for mimo radar waveform design," *IEEE Trans. Aerosp. Electron. Syst.*, vol. 49, no. 2, pp. 1210–1223, APRIL 2013.
- [24] A. De Maio, Y. Huang, and M. Piezzo, "A Doppler robust max-min approach to radar code design," *IEEE Trans. Signal Process.*, vol. 58, no. 9, pp. 4943–4947, Sept 2010.
- [25] M. Naghsh, M. Soltanalian, P. Stoica, M. Modarres-Hashemi, A. De Maio, and A. Aubry, "A Doppler robust design of transmit sequence and receive filter in the presence of signal-dependent interference," *IEEE Trans. Signal Process.*, vol. 62, no. 4, pp. 772–785, Feb 2014.
- [26] P. Stoica and Y. Selen, "Cyclic minimizers, majorization techniques, and the expectation-maximization algorithm: a refresher," *IEEE Signal Process. Mag.*, vol. 21, no. 1, pp. 112–114, Jan 2004.
- [27] Z.-Q. Luo, W.-K. Ma, A.-C. So, Y. Ye, and S. Zhang, "Semidefinite relaxation of quadratic optimization problems," *IEEE Signal Process. Mag.*, vol. 27, no. 3, pp. 20–34, May 2010.
- [28] T. Roh and L. Vandenberghe, "Discrete transforms, semidefinite programming, and sum-of-squares representations of nonnegative polynomials," *SIAM Journal on Optimization*, vol. 16, no. 4, pp. 939–964, 2006.
- [29] S. Boyd and L. Vandenberghe, *Convex optimization*. Cambridge, U.K.: Cambridge University Press, 2004.
- [30] M. Grant and S. Boyd, "CVX: Matlab software for disciplined convex programming, version 2.0 beta," <http://cvxr.com/cvx>, Sep. 2013.
- [31] A. De Maio, S. De Nicola, Y. Huang, Z.-Q. Luo, and S. Zhang, "Design of phase codes for radar performance optimization with a similarity constraint," *IEEE Trans. Signal Process.*, vol. 57, no. 2, pp. 610–621, Feb 2009.
- [32] S. Karbasi, A. Aubry, A. De Maio, and M. Bastani, "Robust transmit code and receive filter design for extended targets in clutter," *IEEE Trans. Signal Process.*, vol. 63, no. 8, pp. 1965–1976, April 2015.
- [33] Y. Huang and D. Palomar, "Rank-constrained separable semidefinite programming with applications to optimal beamforming," *IEEE Trans. Signal Process.*, vol. 58, no. 2, pp. 664–678, Feb 2010.